Electronic Supplementary Material (ESI) for Journal of Materials Chemistry C.

Supplementary Information

for

Coronene Derivatives for Transparent Organic Photovoltaics through Inverse Materials Design

Jeni C. Sorli,[a] Pascal Friederich,[b] Benjamin Sanchez-Langeling,[b] Nick Davy,[a] Guy Olivier Ngongang Ndjawa,[a] Hannah Smith,[c] Xin Lin,[c] Steven Lopez,[b] Melissa Ball,[a,d] Antoine Kahn,[c] Alan Aspuru-Guzik,[b] and Yueh-Lin Loo[a,d]

[a] *Department of Chemical and Biological Engineering, Princeton University, Princeton, NJ, 08544 USA*
[b] *University of Toronto, Toronto, Ontario, Canada*
[c] *Department of Electrical Engineering, Princeton University, Princeton, NJ, 08544 USA*
[d] *Andlinger Center for Energy and the Environment, Princeton University, Princeton, NJ, 08544 USA*

Table of Contents:

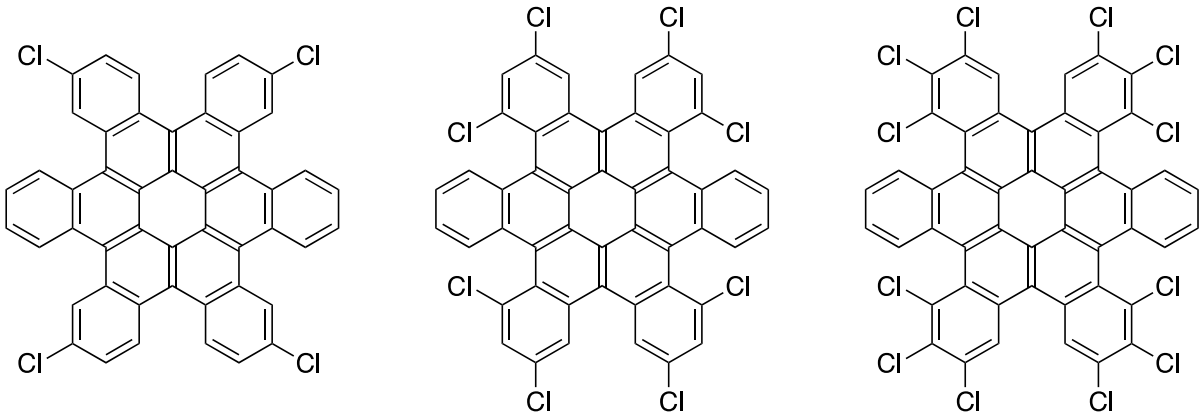

4Cl-cHBC **8Cl-cHBC** **12Cl-cHBC**

Figure S1. Molecular structure of chlorinated contorted hexabenzocoronene derivatives developed by Hiszpanski et al. and used as acceptors in transparent solar cells in this study[1].

a.

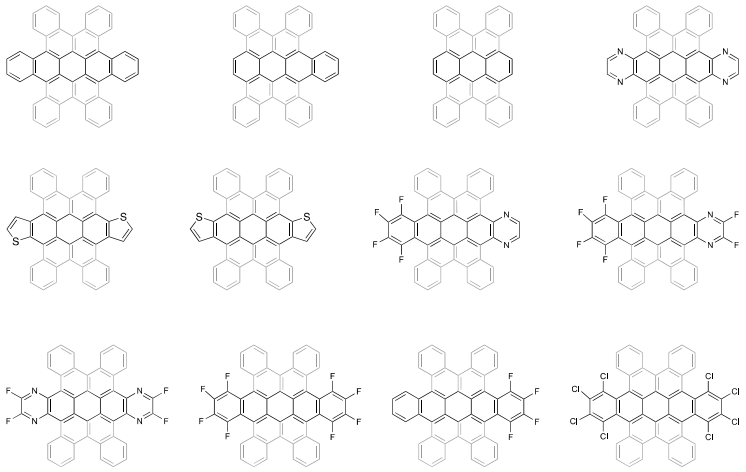

b.

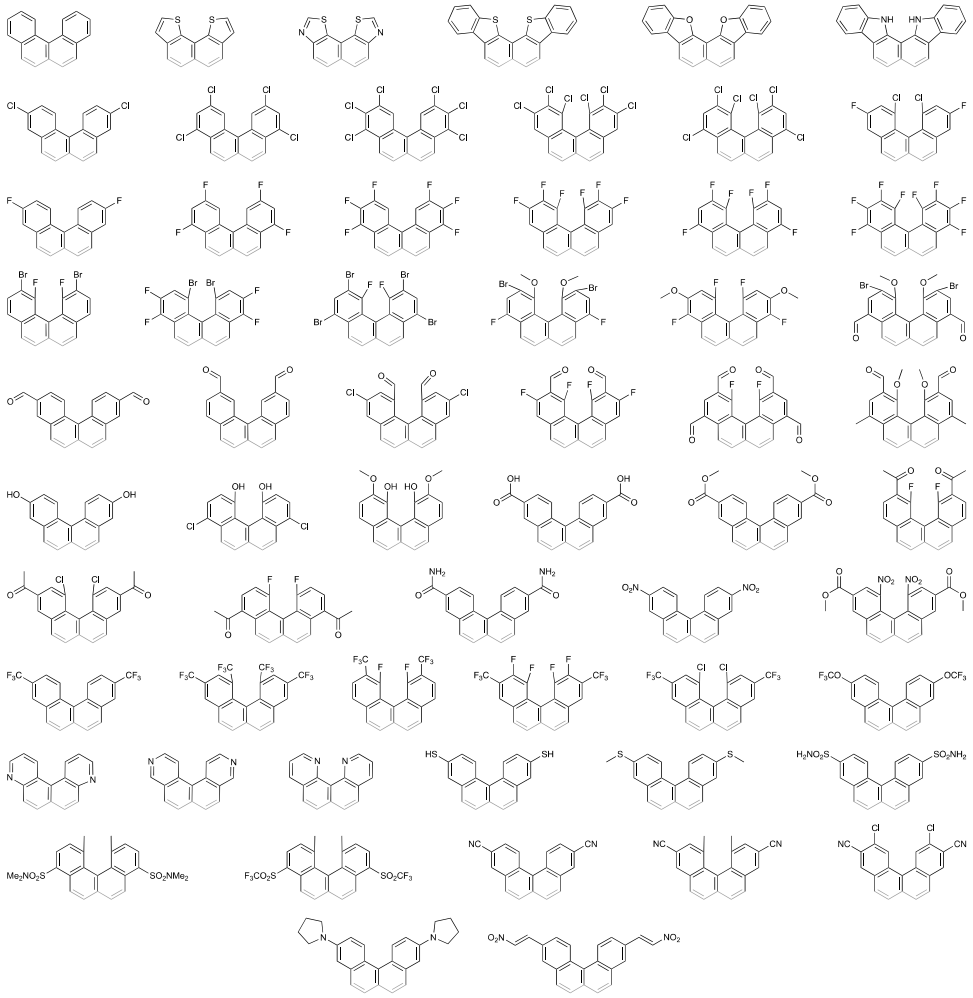

Figure S2. (a) Benzoquinone starting materials and (b) Suzuki substituent fragments used in this study.

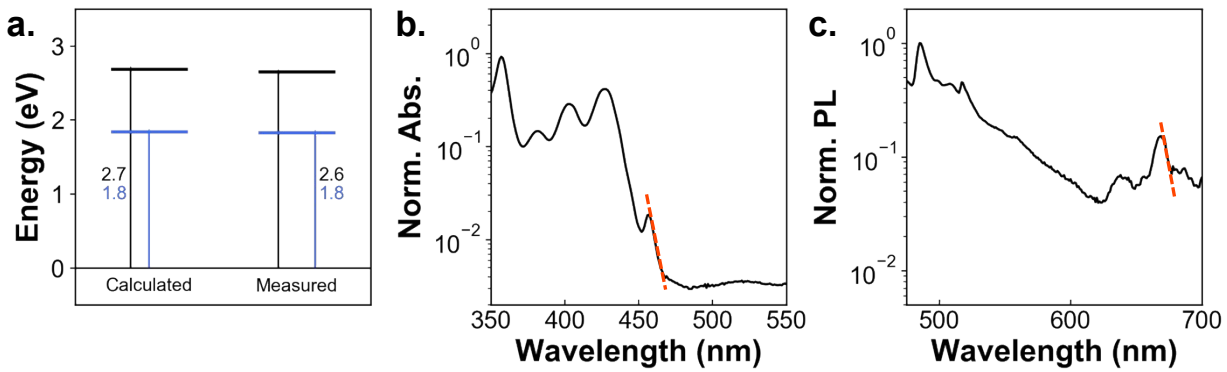

Figure S3. (a) Transition energies for cTBC as calculated, left, and measured via UV-Vis ($S_0 \rightarrow S_1$, black) and low-temperature PL ($S_0 \rightarrow T_n$, blue), right. (b) Solution UV-vis spectra of cTBC in o-DCB with lowest energy feature used for determination of the $S_0 \rightarrow S_1$ highlighted with red dashed line. (c) Low-temperature PL of cTBC dispersed in a polystyrene matrix with lowest energy feature used to determine the $S_0 \rightarrow T_n$ transition highlighted with red dashed line.

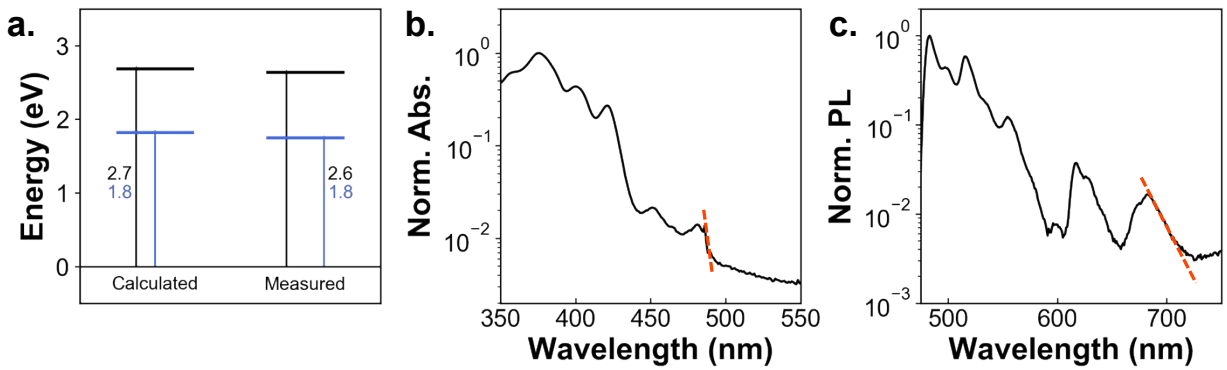

Figure S4. (a) Transition energies for cPBC as calculated, left, and measured via UV-Vis ($S_0 \rightarrow S_1$, black) and low-temperature PL ($S_0 \rightarrow T_n$, blue), right. (b) Solution UV-vis spectra of cPBC in o-DCB with lowest energy feature used for determination of the $S_0 \rightarrow S_1$ highlighted with red dashed line. (c) Low-temperature PL of cPBC dispersed in a polystyrene matrix with lowest energy feature used to determine the $S_0 \rightarrow T_n$ transition highlighted with red dashed line.

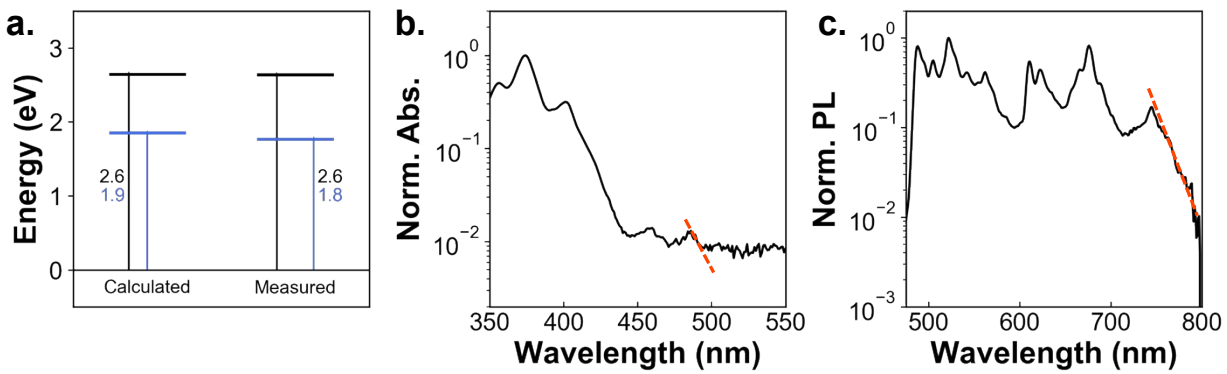

Figure S5. (a) Transition energies for cHBC as calculated, left, and measured via UV-Vis ($S_0 \rightarrow S_1$, black) and low-temperature PL ($S_0 \rightarrow T_n$, blue), right. (b) Solution UV-vis spectra of cHBC in o-DCB with lowest energy feature used for determination of the $S_0 \rightarrow S_1$ highlighted with red dashed line[1]. (c) Low-temperature PL of cHBC dispersed in a polystyrene matrix with lowest energy feature used to determine the $S_0 \rightarrow T_n$ transition highlighted with red dashed line.

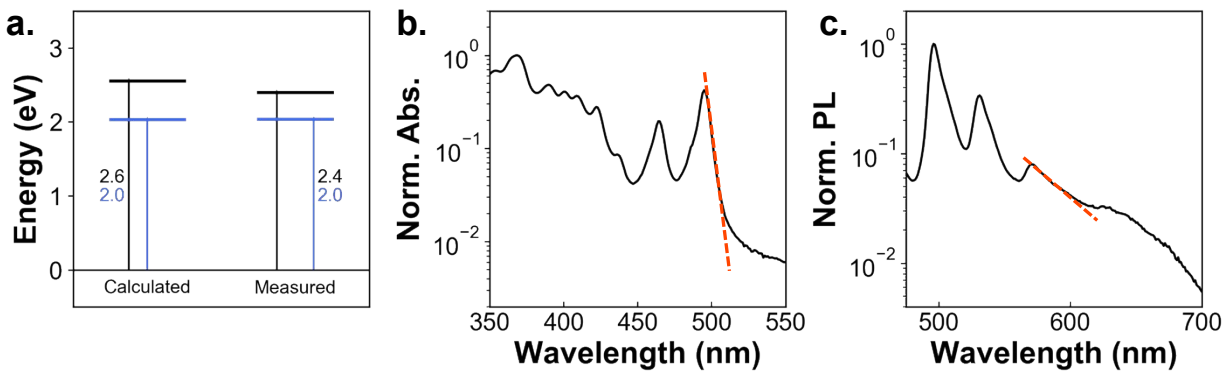

Figure S6. (a) Transition energies for cTBFBC as calculated, left, and measured via UV-Vis ($S_0 \rightarrow S_1$, black) and low-temperature PL ($S_0 \rightarrow T_n$, blue), right. (b) Solution UV-vis spectra of cTBFBC in o-DCB with lowest energy feature used for determination of the $S_0 \rightarrow S_1$ highlighted with red dashed line. (c) Low-temperature PL of cTBFBC dispersed in a polystyrene matrix with lowest energy feature used to determine the $S_0 \rightarrow T_n$ transition highlighted with red dashed line.

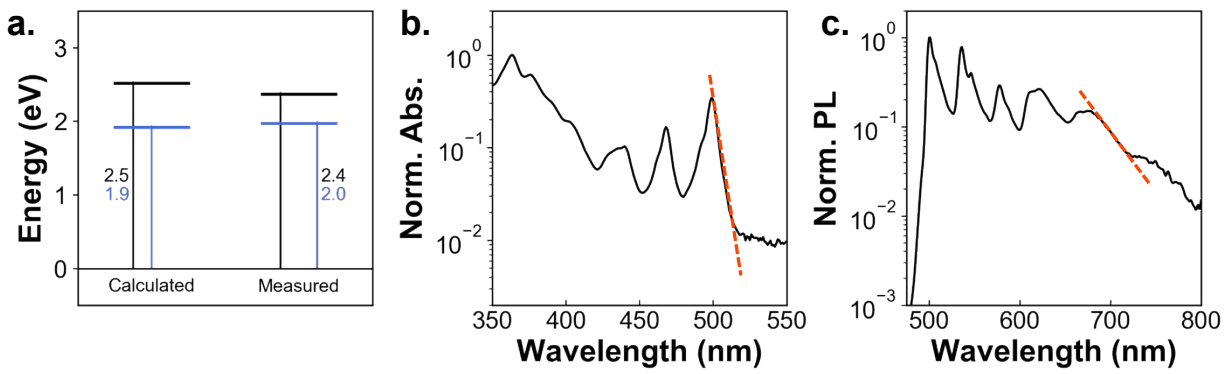

Figure S7. (a) Transition energies for cTBFDBC as calculated, left, and measured via UV-Vis ($S_0 \rightarrow S_1$, black) and low-temperature PL ($S_0 \rightarrow T_n$, blue), right. (b) Solution UV-vis spectra of cTBFDBC in o-DCB with lowest energy feature used for determination of the $S_0 \rightarrow S_1$ highlighted with red dashed line. (c) Low-temperature PL of cTBFDBC dispersed in a polystyrene matrix with lowest energy feature used to determine the $S_0 \rightarrow T_n$ transition highlighted with red dashed line.

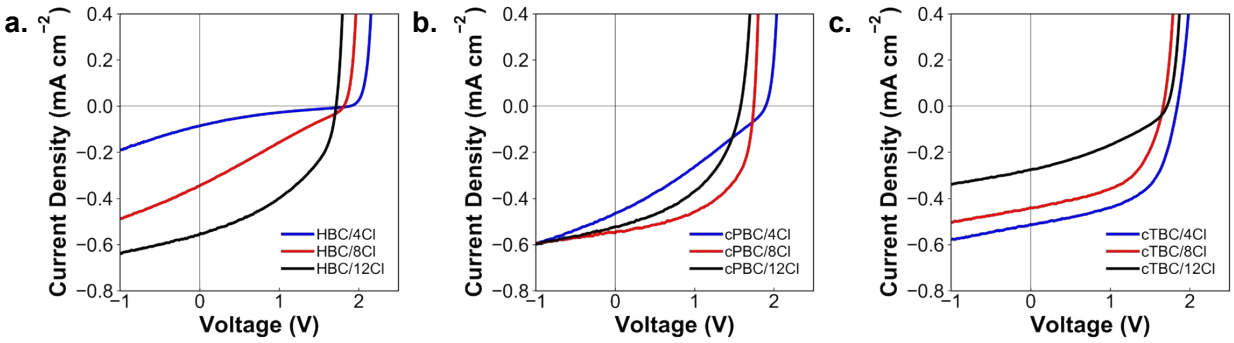

Figure S8. J-V characteristics for (a) cHBC, (b) cPBC, and (c) cTBC bilayer devices with 4Cl-cHBC (blue), 8Cl-cHBC (red) and 12Cl-cHBC (black).

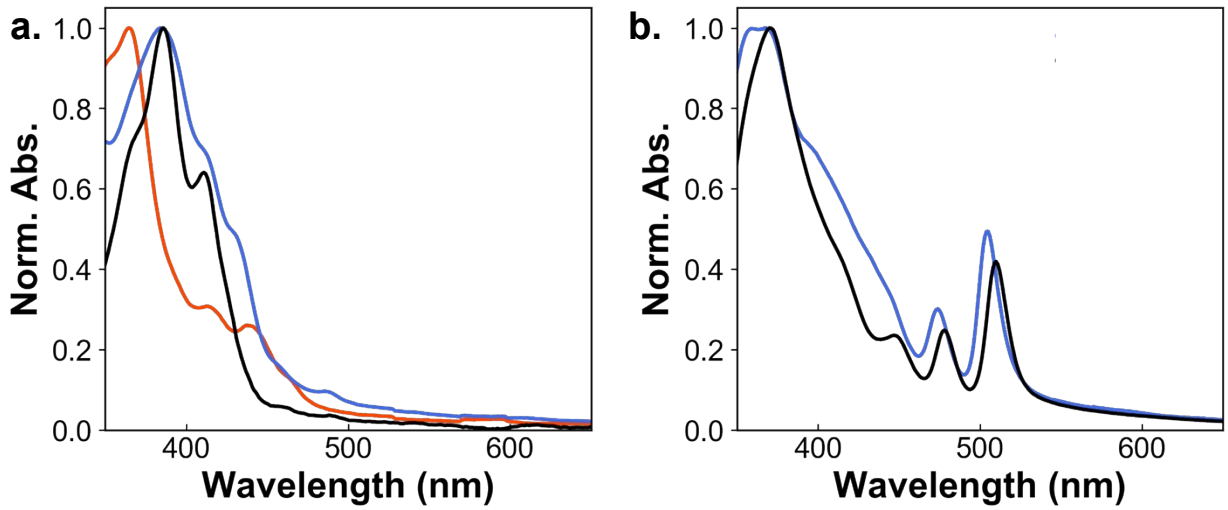

Figure S9. Normalized UV-Vis absorption for solid-state amorphous films of (a) phenyl derivatives and (b) benzofuranyl derivatives. In (a) cTBC is plotted in orange, cPBC is plotted in blue and cHBC is plotted in black. In (b) cTBFBC is plotted in blue and cTBFDBC is plotted in black.

Calculation Details

Computational details followed previously established protocols to enable comparisons with previous data sets[2]. A conformer search was performed using the semiempirical method CREST[3]. Each of the 20 lowest energy molecular conformers were then relaxed using DFT with the BP86 functional[4] and the def2-SVP basis set[5]. Duplicate conformers were removed and single point calculations of the remaining conformers were performed using a B3LYP[6]/def2-SVP level of theory, followed by Boltzmann averaging of the resulting HOMO and LUMO energy levels. Excited state transitions were then calculated at the same level of theory on the lowest-energy conformer using time-dependent density functional theory (TDDFT) to obtain the S_0-S_1, S_0-T_1 and S_0-T_2 transition energies.

Substrate Preparation

For UV-visible measurements, glass slides were cleaned by sonication in deionized water, acetone, and isopropyl alcohol and then dried with nitrogen prior to film deposition. Glass substrates (23 mm × 27 mm) pre-patterned with an ITO strip 7.5 mm wide and 23 mm long (20 Ω/square, TFD) were cleaned by sonication in detergent, deionized water, acetone, and isopropyl alcohol, and then dried with nitrogen. They were then subjected to a UV-ozone treatment for 10 minutes before immediate transfer to a nitrogen glove box for deposition of the coronene derivatives. Unpatterned ITO on glass was used for UPS/IPES measurements and were cleaned using the same procedure described for ITO substrates above.

Materials Characterization

Optical Characterization

UV-visible solid-state spectra were collected on samples evaporated on glass slides and measured using an Agilent Technologies Cary 5000 spectrophotometer. UV-visible solution measurements were performed on dilute solutions (filtered due to low solubility) in ortho-dichlorobenzene using an Agilent Technologies Cary 5000 spectrophotometer. The $S_0 \rightarrow S_1$ transition energy was obtained by extracting the onset energy of the lowest energy absorption feature by finding the linear intersection with the baseline absorption.

Samples for photoluminescence experiments were prepared in carbon disulfide by diluting a saturated solution, obtained through sonication and filtering out the solids, until a solution with optical density of 0.5 through UV-Vis was obtained. 20 uL of the resulting solution was added to a 2 mL polystyrene solution, which was then cast into films on glass slides. The polystyrene stock solution was made at a concentration of 6 mg/mL, using polystyrene with a molar mass of 300 kDa. The samples were then cooled to low temperature using liquid nitrogen and spectra were collected using an Edinburgh Instruments FLS980 spectrophotometer. Similarly to the $S_0 \rightarrow S_1$ transition, the energy for the $S_0 \rightarrow T_n$ transition was extracted by finding energy of the lowest energy peak feature.

Electrical Characterization

Ultraviolet photoelectron spectroscopy (UPS) and inverse photoemission spectroscopy (IPES) experiments were conducted in an ultrahigh-vacuum chamber with a base pressure of 5×10^{-10} Torr. UPS measurements were done with both the He I (21.22 eV) and He II (40.81 eV) photon lines generated by a discharge lamp. IPES was performed in the isochromat mode with a setup described elsewhere[7]. The nominal energy resolutions for UPS and IPES were 100 meV,

and 400 meV, respectively. Materials were prepared by thermal evaporation at a rate of 2 Å s^{-1} onto glass/ITO substrates under vacuum to a thickness of 10 nm.

Device Preparation and Testing

MoO_3 (99.97%, Sigma-Aldrich) and bathocuproine (BCP, 99.99%, Sigma-Aldrich) were used as-received. We evaporated 5 nm of MoO, 23 nm of coronene derivative donor, 17 nm of coronene derivative acceptor, and 5 nm of BCP sequentially onto prepatterned ITO at a pressure of 1×10^{-6} Torr. Then, 100 nm of aluminum was thermally evaporated through patterned masks that defined the active layer at 0.18 cm^2. The devices were measured under AM1.5G 100 mW/cm^2 illumination in a nitrogen-filled glovebox and the current density−voltage (J−V) characteristics were acquired with a Keithley 2400 source measurement unit. For each donor/acceptor pair, a minimum of 10 devices were fabricated and measured.

General Synthetic Information

cHBC, cTBFDBC, 4Cl-cHBC, 8Cl-cHBC and 12Cl-cHBC were synthesized according to previously reported methods[1,8,9]. 9,10-anthraquinone, 5,12-naphthacenequinone, carbon tetrabromide, triphenylphosphine, bis(tripheylphosphine) palladium(II) dichloride, potassium phosphate tribasic, phenylboronic acid, iodine, iron (III) chloride, propylene oxide, dioxane, and nitromethane were purchased from Sigma Aldrich and were used as-received without further purification. All reactions were run in oven-dried glassware (130°C). Flasks were fitted with rubber septa and reactions were conducted under a positive pressure of nitrogen unless otherwise noted. Column chromatography was performed on a CombiFlash® Rf system using RediSepTM normal phase silica columns (ISCO, Inc.). ^{1}H and ^{13}C NMR spectra were collected on Bruker DRX spectrometers at room temperature operating at 500 MHz and 126 MHz, respectively. All peaks are reported as δppm. ^{13}C NMR could not be obtained for 5, 9, 10, or 12 due to low solubility of the materials. HRMS were collected on an Agilent 7200 GC/QTOF.

Synthetic Procedures and Characterization Data

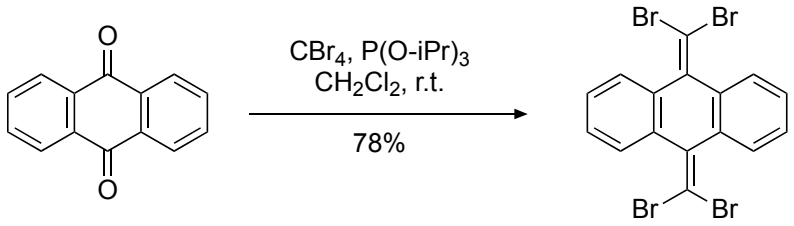

1 **2**

Synthesis of (2) 9,10-bis(dibromomethylene)-9,10-dihydroanthracene (Corey Fuchs Reaction)

Carbon tetrabromide (1990 mg, 6.0 mmol) and 9,10-anthraquinone (500 mg, 2.4 mmol) were added to a 250 mL three-necked round-bottom flask with a stir bar and sealed with rubber septa. The flask and solids were purged with vacuum/N2 cycling, and 120 mL were then added to the flask under nitrogen. The suspension was then stirred under nitrogen on ice for 30 minutes. Triisopropyl phosphite (4.4 mL, 19.2 mmol) and anhydrous DCM (5 mL) were added to a purged vial sealed with a septum and then introduced to the suspension over ice by syringe drop-wise over the course of 20-30 minutes. During the course of the addition, the flask contents changed from a white-yellow suspension to a dark brown solution. The solution was then removed from the ice bath and stirred for 12 hours under nitrogen. The reaction was then quenched with methanol, which was followed with removal of approximately 100 mL of DCM via rotovap. The removal of DCM and the subsequent cooling of the reaction flask after rotovapping induced crystallization of the final product, which produced needle-like, pale yellow crystals which were filtered and rinsed with methanol before drying in a vacuum oven, yielding 980 mg of product (78% yield). ^{1}H NMR (500 MHz, Methylene Chloride-d_2) δ 7.85 (dd, J = 5.7, 3.3 Hz, 4H), 7.32 (dd, J = 5.8, 3.3 Hz, 4H). ^{13}C NMR (126 MHz, Chloroform-d) δ 139.69, 136.06, 127.85, 127.22, 90.56. Primary m/z peak calculated $C_{16}H_8Br_4$: 515.74, found: 515.77.

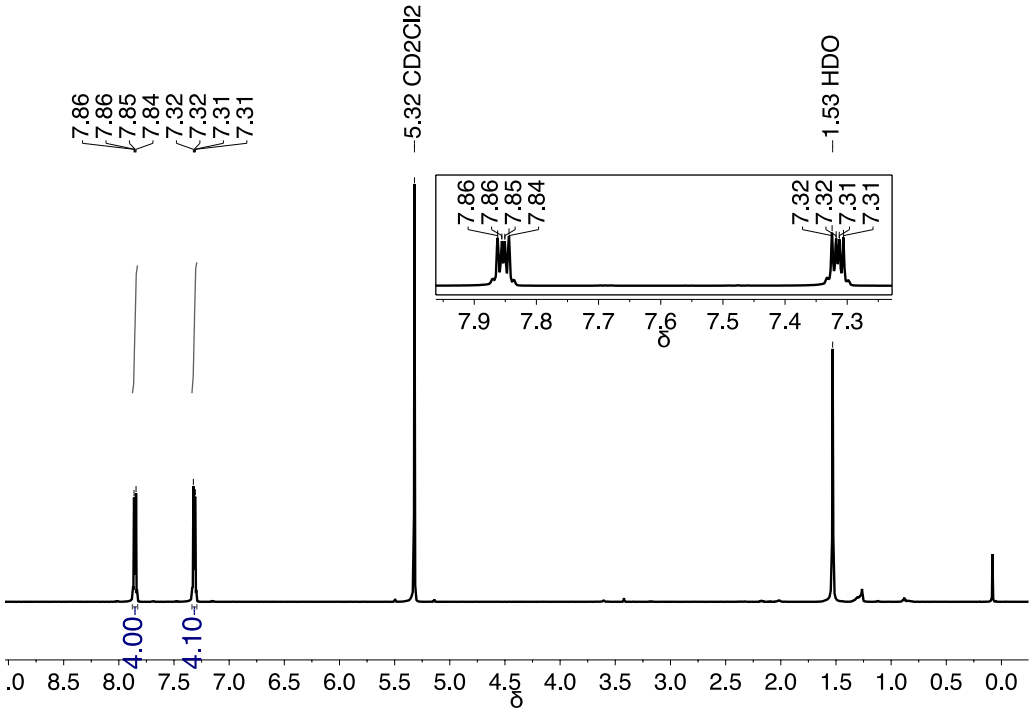

Figure S10. ^{1}H NMR of 9,10-bis(dibromomethylene)-9,10-dihydroanthracene (2). Peaks assigned to molecule have been expanded in the inset figure.

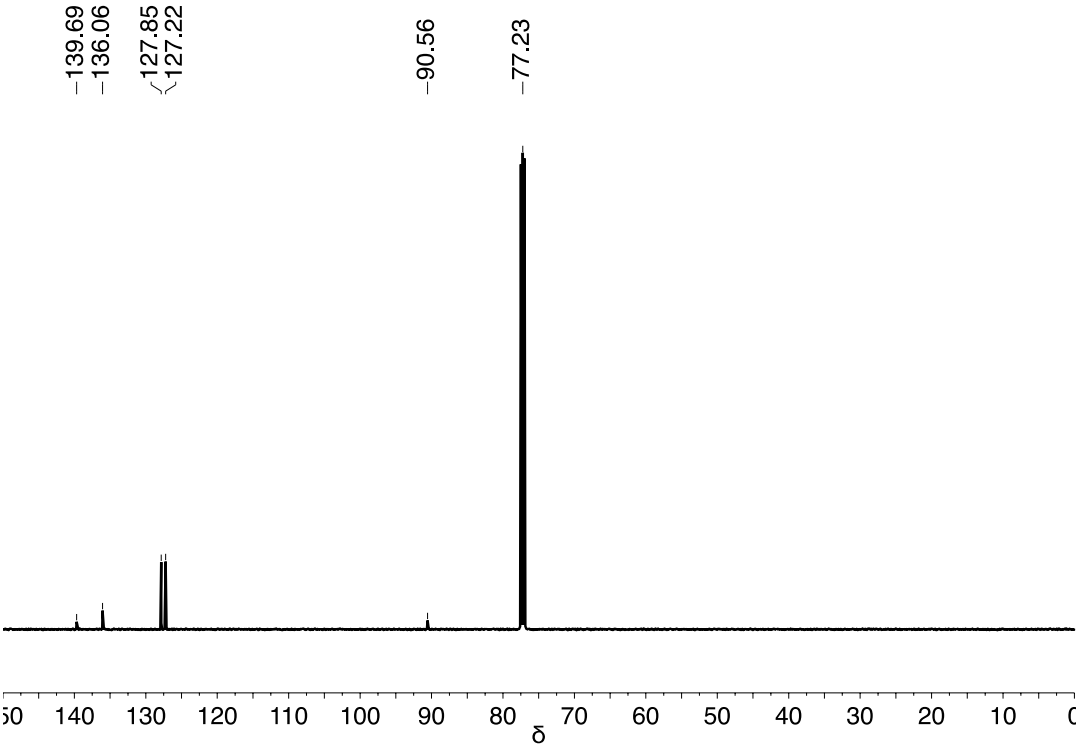

Figure S11. ^{13}C NMR of 9,10-bis(dibromomethylene)-9,10-dihydroanthracene (2).

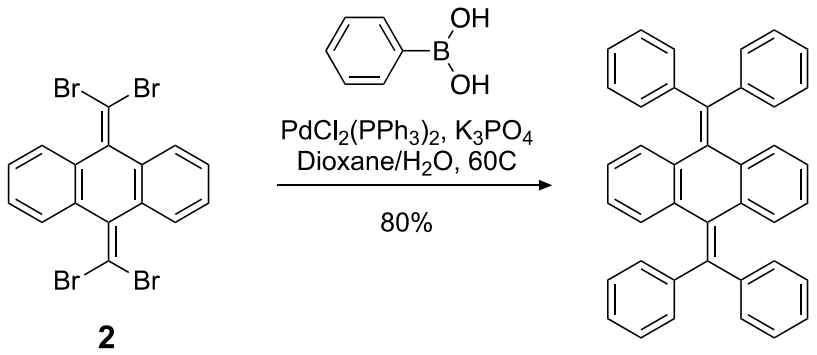

2 **3**

Synthesis of (3) 9,10-bis(diphenylmethylene)-9,10-dihydroanthracene (Suzuki coupling)

(210 mg, 0.4 mmol) of **2**, (54 mg, 0.1 mmol) bis(triphenylphosphine)palladium(II) dichloride, and (246 mg, 2 mmol) phenylboronic acid were added to a nitrogen-purged, 25 mL roundbottom flask and purged with nitrogen. Dioxane (6 mL) was added via syringe to the roundbottom flask and sparged with nitrogen for 20 minutes. (645 mg, 3 mmol) tribasic postassium phosphate were added to a 20 mL vial and sealed with a septum. 2 mL of distilled H2O were added via syringe to the vial containing the base and were sparged with nitrogen for 20 minutes. The vial was then lowered into a silicon oil bath heated to 60C, and the base solution was added via needle through the septa. The solution was sparged for 5 minutes before the inlet and outlet were removed and the reaction was stirred overnight. The reaction was stopped when **2** was consumed (verified by TLC hexanes/DCM 3:1) and the solution became brown. The product was then extracted with dichloromethane, separated from the aqueous phase, washed with brine solution, and extracted with dichloromethane and separated again. The organic phase was then dried via rotovap and purified using flash column chromatography (hexane/DCM 3:1) to isolate 165 mg (80%) of **3**. ^{1}H NMR (500 MHz, Methylene Chloride-d_2) δ 7.43 (d, J = 7.3 Hz, 8H), 7.32 (t, J = 7.6 Hz, 8H), 7.23 (t, J = 7.4 Hz, 4H), 7.01 (dd, J = 5.7, 3.3 Hz, 4H), 6.72 (dd, J = 5.8, 3.3 Hz, 4H). ^{13}C NMR (126 MHz, Methylene Chloride-d_2) δ 143.19, 140.60, 138.35, 135.84, 130.11, 128.80, 128.45, 127.25, 125.62. Primary m/z peak calculated $C_{40}H_{28}$: 508.22, found: 508.23.

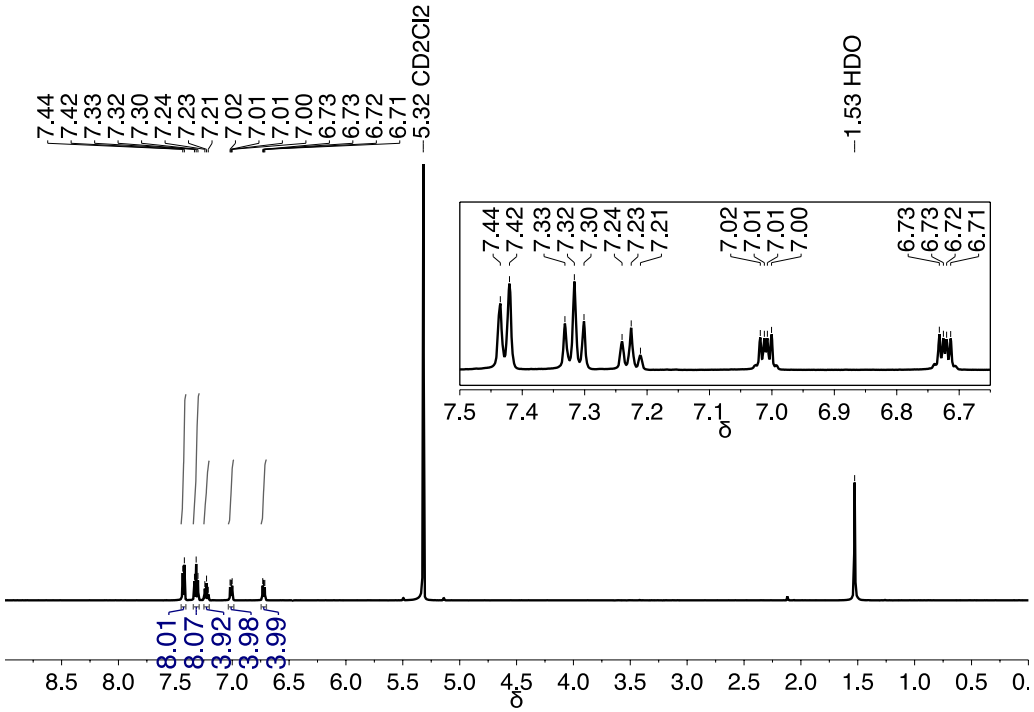

Figure S12. ^{1}H NMR of 9,10-bis(diphenylmethylene)-9,10-dihydroanthracene (3). Peaks assigned to molecule have been expanded in the inset figure.

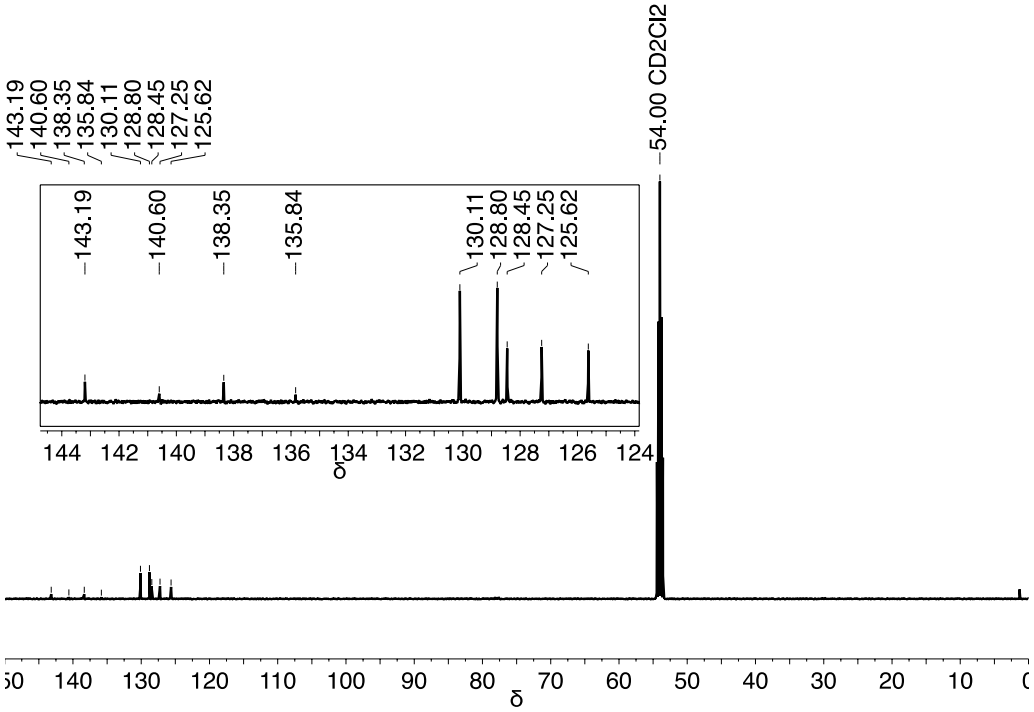

Figure S13. ^{13}C NMR of 9,10-bis(diphenylmethylene)-9,10-dihydroanthracene (3). Peaks assigned to molecule have been expanded in the inset figure.

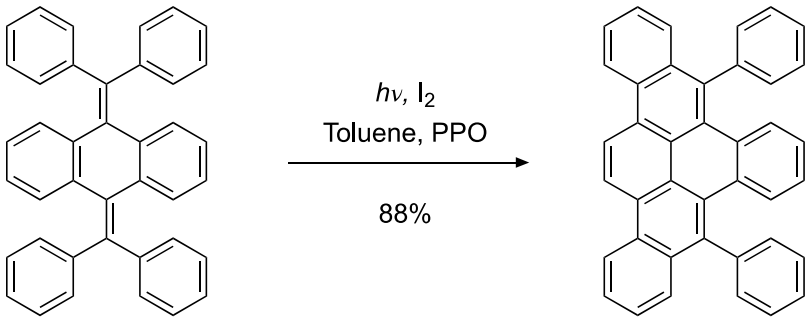

3 **4**

Synthesis of (4) 5,10-diphenyldibenzopentaphene (Photocyclization)

(150 mg, 0.3 mmol) of **3** were added to a 500 mL flat-bottomed and 400 mL of toluene and sonicated, yielding a clear solution. (525 mg, 2 mmol) of iodine were added to the photoreaction glassware and about 100 mL of toluene were added to the vessel with a nitrogen bubbler and sparged until the iodine fully dissolved. The solution of **3** in toluene was added to the photoreaction glassware and was bubbled with nitrogen for 20 min. 20 mL of propylene oxide were added and the UV lamp was turned on. The reaction ran for 2 hours with a nitrogen purge, and TLC confirmed that **3** was no longer present. TLC with hexanes/DCM (3:1) showed the presence of blue fluorescence, which indicated the half-cyclized product (4). The reaction volume was rotovapped to approximately 50 mL, and the product was precipitated with the addition of methanol, which was then filtered and rinsed with methanol and dried in the vacuum oven, yielding 132 mg of yellow powder (88%). ^{1}H NMR (500 MHz, Methylene Chloride-d_2) δ 9.19 (s, 2H), 9.06 (d, J = 8.3 Hz, 2H), 8.05 (d, J = 8.4 Hz, 2H), 7.80 (t, J = 7.4 Hz, 2H), 7.65 (t, J = 9.3 Hz, 5H), 7.60 (t, J = 7.5 Hz, 4H), 7.55 (d, J = 7.3 Hz, 2H), 7.52 (dd, J = 6.2, 3.4 Hz, 2H), 6.77 (dd, J = 6.3, 3.4 Hz, 2H). ^{13}C NMR (126 MHz, $CDCl_3$) δ 133.80, 132.67, 130.87, 129.74, 129.19, 127.83, 127.67, 126.70, 126.44, 125.62, 123.08, 121.92. Primary m/z peak calculated $C_{40}H_{24}$: 504.19, found: 504.17.

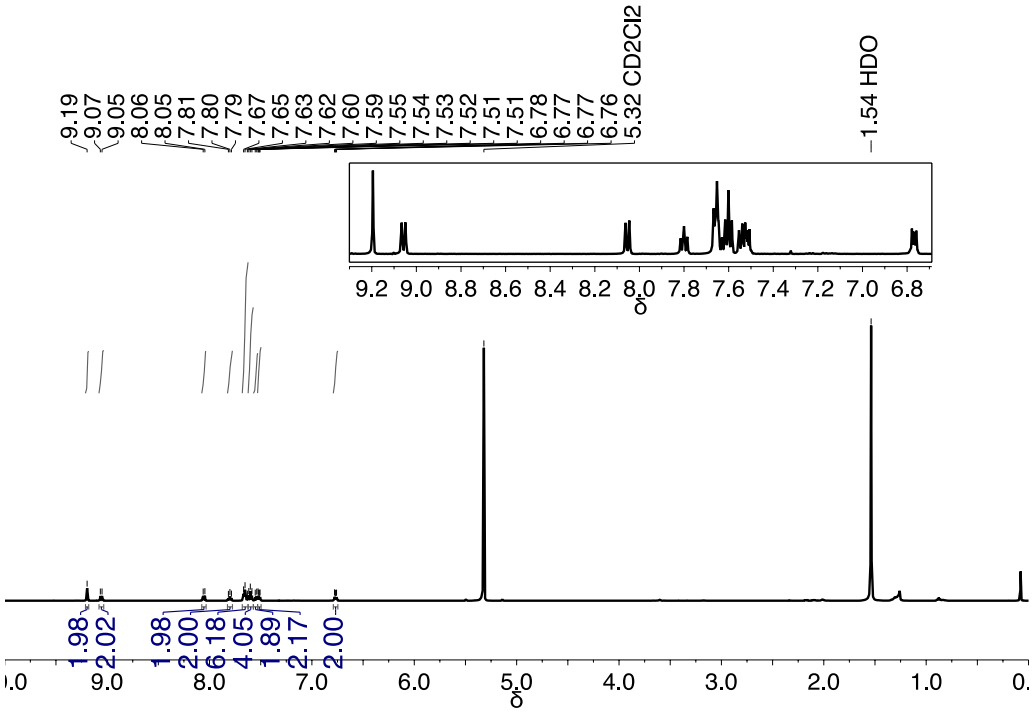

Figure S14. ^{1}H NMR of 5,10-diphenyldibenzopentaphene (4). Peaks assigned to molecule have been expanded in the inset figure.

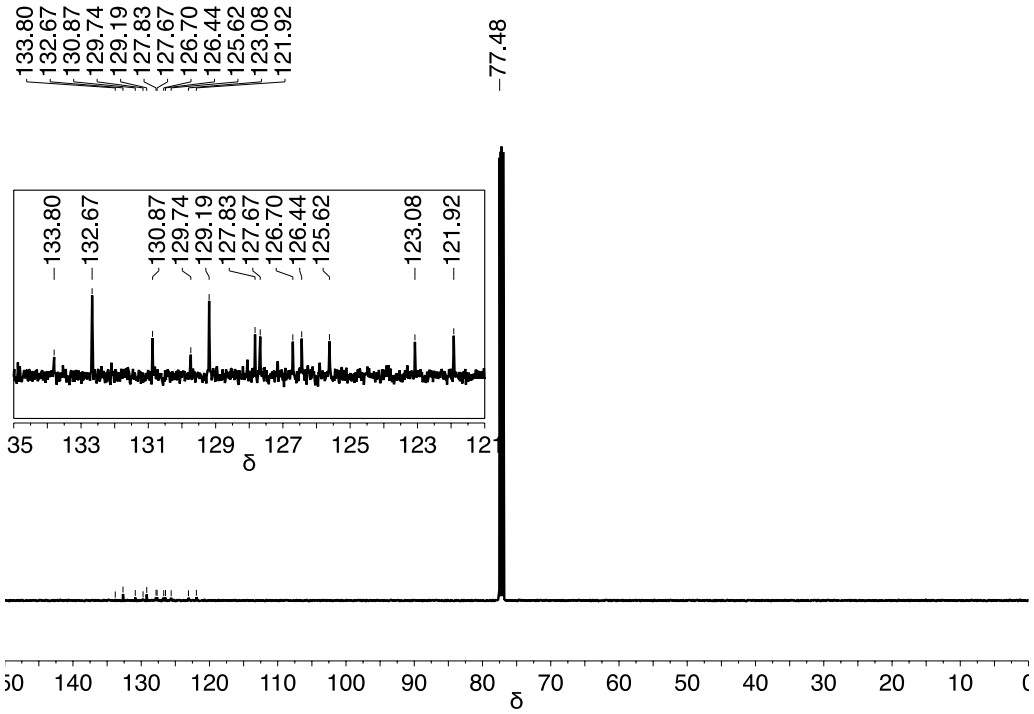

Figure S15. ^{13}C NMR of ^{1}H NMR of 5,10-diphenyldibenzopentaphene (4). Peaks assigned to molecule have been expanded in the inset figure.

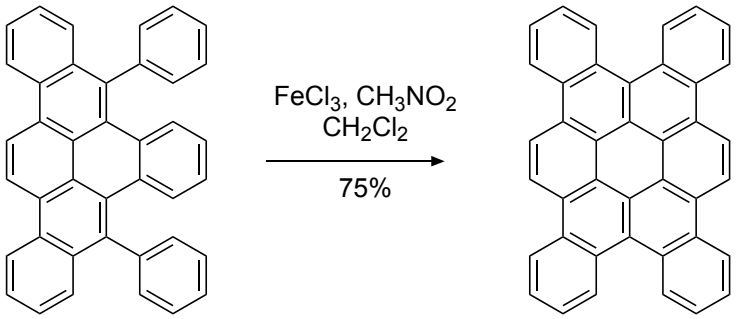

4 **5**

Synthesis of (5) tetrabenzocoronene (Scholl Reaction)

130 mg (0.25 mmol) of **4** was dissolved in 130 mL of DCM (1mg/mL) and the solution was sealed in a 250 mL round-bottom flask with a rubber septum and stir bar and sparged. Iron (III) chloride (334 mg, 2 mmol) was dissolved in a minimal amount of nitromethane (2.5 mL) and was added dropwise to the flask while stirring, which resulted in a change from a yellow solution to a dark green solution. The reaction was monitored by TLC (hexanes/DCM 3:1) until there was no blue fluorescence remaining from **4** and only green fluorescence from **5** remained, which took approximately 1 hour. The reaction was quenched with methanol, which also precipitated the final product, **5**. The product was filtered and rinsed with methanol before drying in a vacuum oven, yielding 95 mg (75%). ^{1}H NMR (500 MHz, Tetrachloroethane-d_2) δ 9.50 (s, 3H), 9.31 (d, J = 8.2 Hz, 4H), 9.27 (d, J = 7.8 Hz, 4H), 8.00 (t, J = 7.4 Hz, 4H), 7.92 (t, J = 7.6 Hz, 4H). Primary m/z peak calculated $C_{40}H_{20}$: 500.16, found: 500.15.

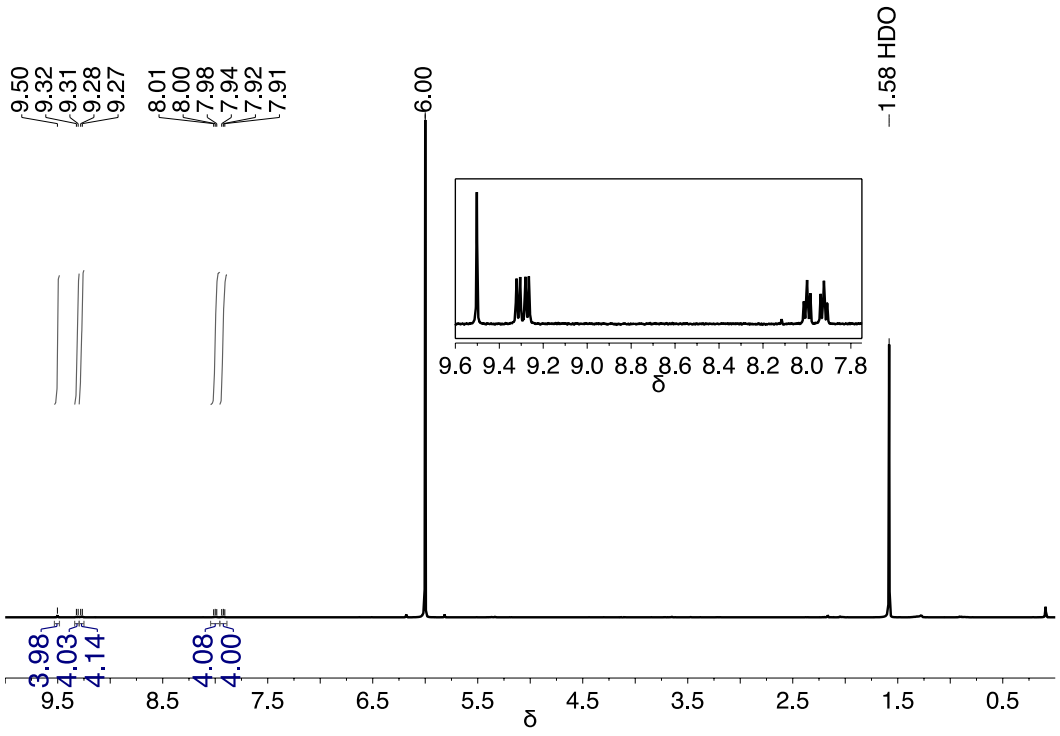

Figure S16. ^{1}H NMR of cTBC (5). Peaks assigned to molecule have been expanded in the inset figure.

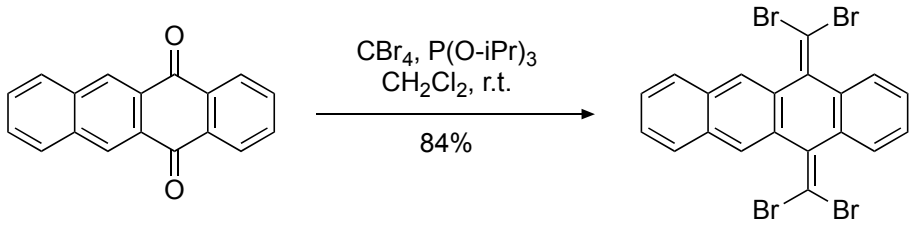

6 **7**

Synthesis of (7) 5,12-bis(dibromomethylene)-5,12-dihydrotetracene

Synthesis of **7** followed the same Corey Fuchs reaction procedure and equivalencies as that used for **2**. Initial reactants of carbon tetrabromide (1605 mg, 4.8 mmol) and 5,12-naphthaquinone (500 mg, 1.9 mmol), which when carried through the same process yielded 932 mg of white-yellow needles (84% yield). ^{1}H (500 MHz, Methylene Chloride-d_2) δ 8.28 (s, 2H), 7.87 (dd, J = 5.9, 3.3 Hz, 4H), 7.53 (dd, J = 6.3, 3.2 Hz, 2H), 7.33 (dd, J = 5.8, 3.3 Hz, 2H). ^{13}C NMR (126 MHz, $CDCl_3$) δ 139.76, 136.20, 133.41, 131.82, 128.30, 127.95, 127.46, 127.36, 127.28, 77.48. Primary m/z peak calculated $C_{20}H_{10}Br_4$: 565.75, found: 565.78.

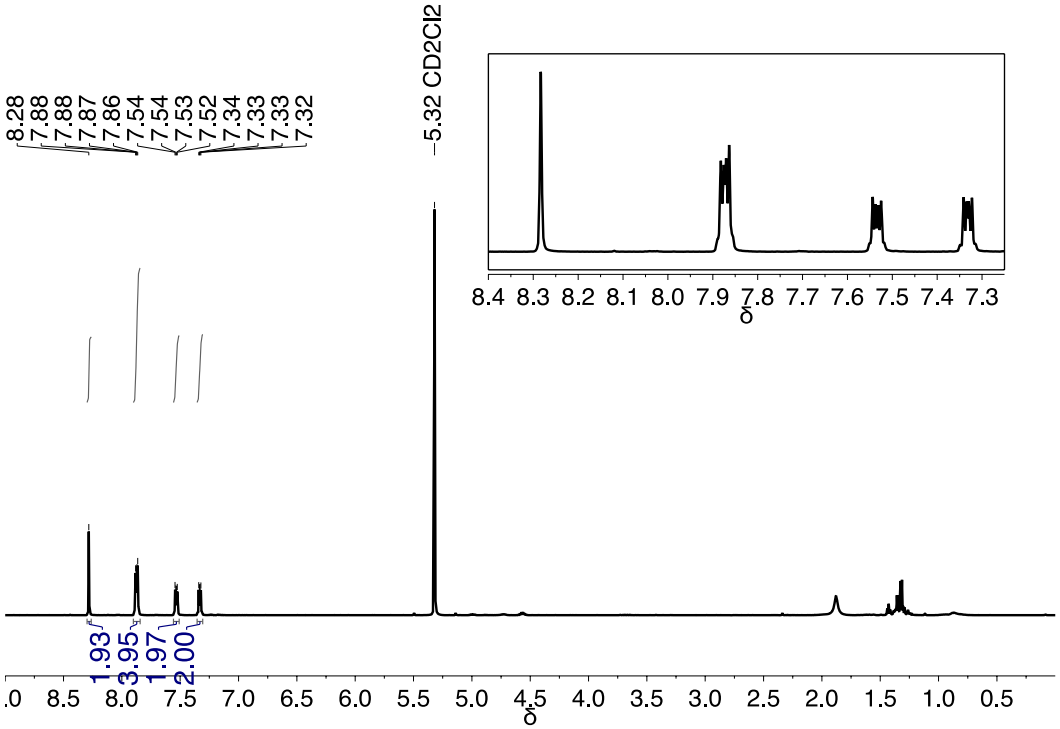

Figure S17. ^{1}H NMR of 5,12-bis(dibromomethylene)-5,12-dihydrotetracene (7). Peaks assigned to molecule have been expanded in the inset figure. Upfield peaks are associated with water and grease. The grease impurity is removed in subsequent processing/columns.

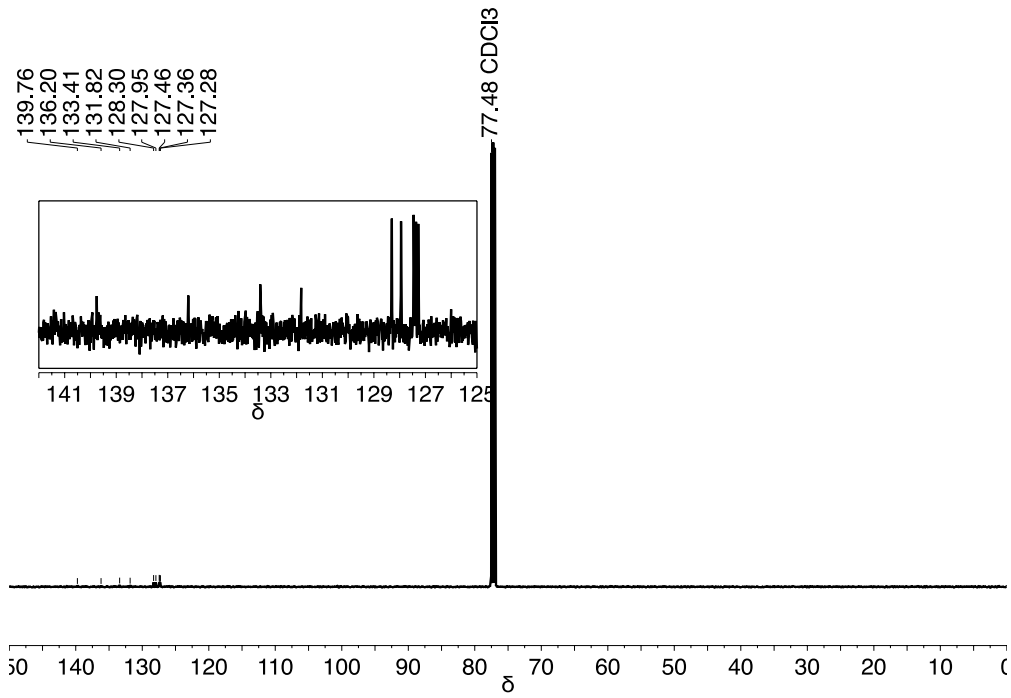

Figure S18. ^{13}C NMR of 5,12-bis(dibromomethylene)-5,12-dihydrotetracene (7). Peaks assigned to molecule have been expanded in the inset figure.

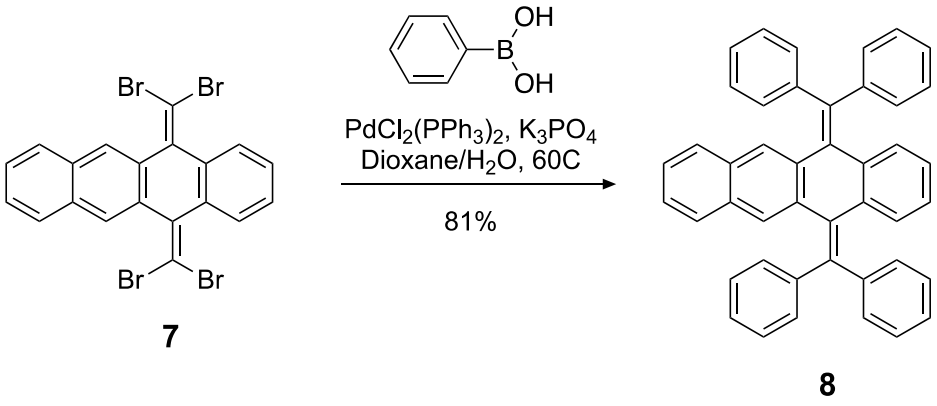

7 **8**

Synthesis of (8) 5,12-bis(diphenylmethylene)-5,12-dihydrotetracene

Synthesis of **8** followed the same Suzuki coupling procedure as that for **3**, above. Starting with 150 mg (0.26 mmol) of **7**, resulted in 120 mg of white powder of **8** after workup (81% yield). ^1H NMR (500 MHz, Methylene Chloride-d_2) δ 7.50 – 7.46 (m, 10H), 7.36 – 7.28 (m, 10H), 7.26 – 7.17 (m, 6H), 7.06 (dd, J = 5.8, 3.3 Hz, 2H), 6.75 (dd, J = 5.8, 3.3 Hz, 2H). ^{13}C NMR (126 MHz, CD_2Cl_2) δ 143.13, 143.10, 141.17, 138.55, 136.25, 135.88, 131.72, 130.16, 130.11, 128.88, 128.80, 128.61, 127.96, 127.35, 127.30, 127.23, 126.21, 125.93. Primary m/z peak calculated $C_{44}H_{30}$: 558.23, found: 558.24.

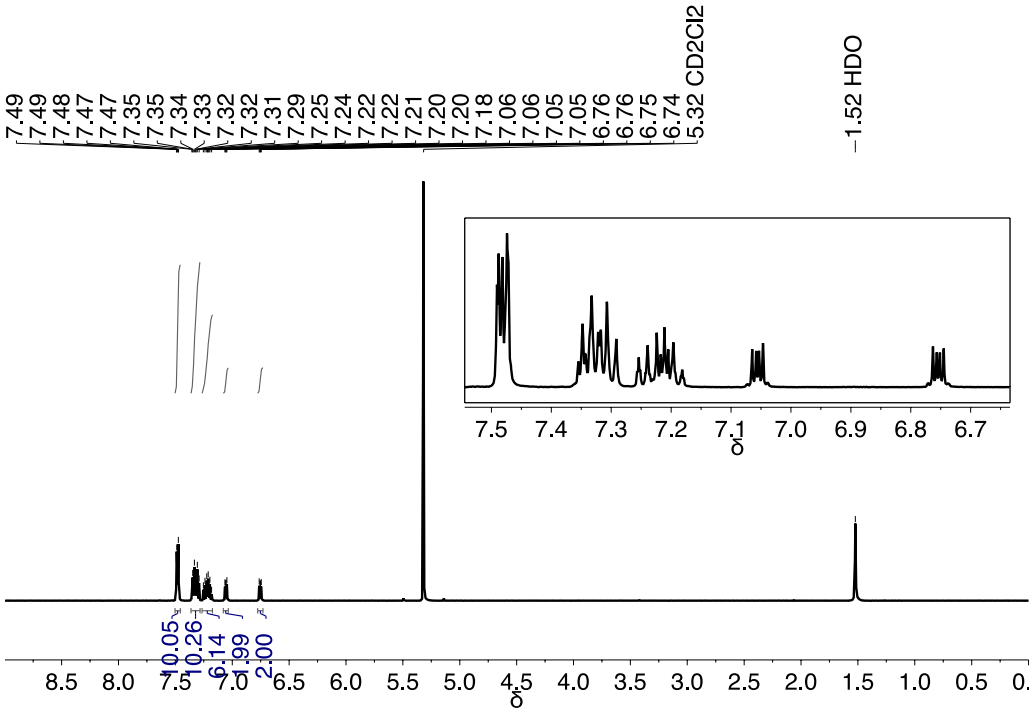

Figure S19. ^{1}H NMR of 5,12-bis(diphenylmethylene)-5,12-dihydrotetracene (8). Peaks assigned to molecule have been expanded in the inset figure.

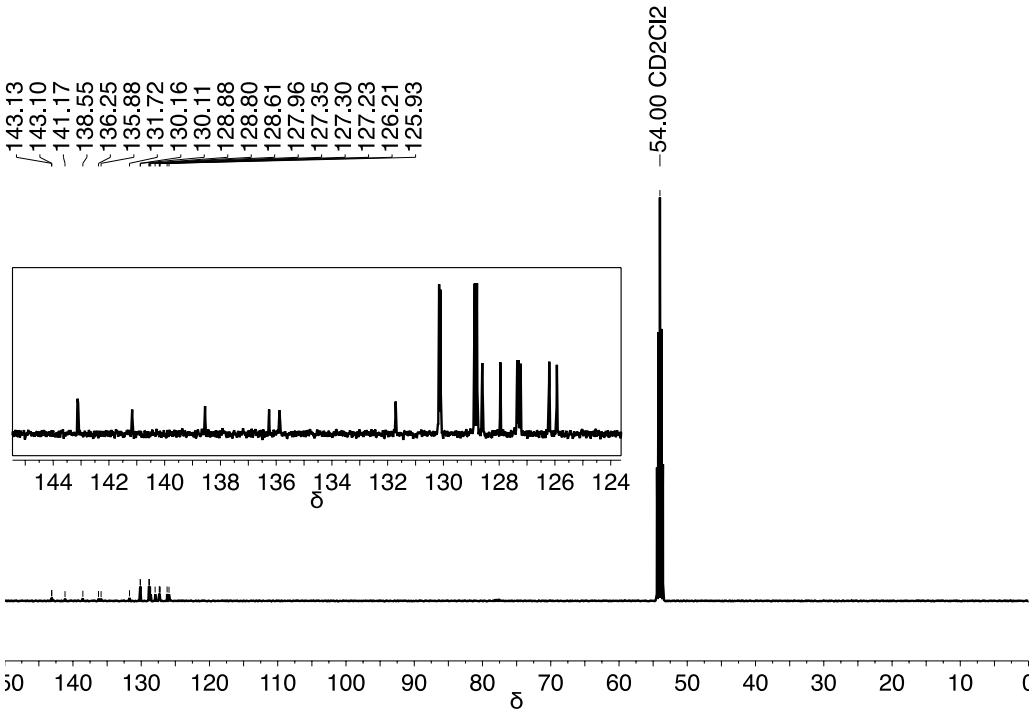

Figure S20. ^{13}C NMR of 5,12-bis(diphenylmethylene)-5,12-dihydrotetracene (8). Peaks assigned to molecule have been expanded in the inset figure.

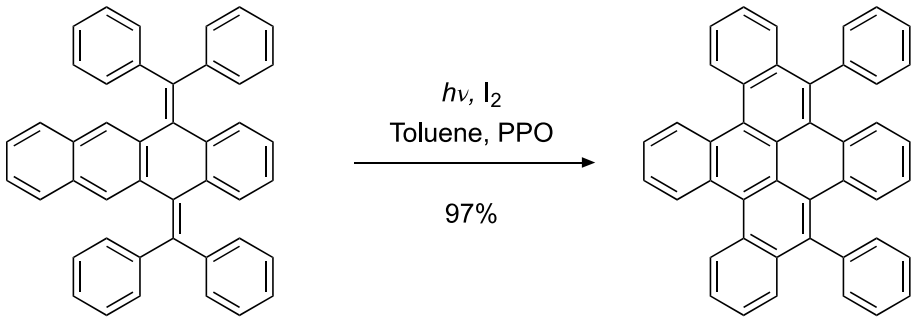

8 **9**

Synthesis of (9) 13,18-diphenylbenzonaphtho[1,2,3,4]pentaphene

Synthesis of **9** followed the same photocyclization procedure as that for **4**, above. Starting with 100 mg (0.18 mmol) of **8**, resulted in 96 mg of yellow powder of **8** after workup (97% yield). ^{1}H NMR (500 MHz, Tetrachloroethane-d_2) δ 9.15 (d, J = 8.5 Hz, 2H), 8.97 (dd, J = 6.1, 3.4 Hz, 2H), 7.90 (d, J = 8.5 Hz, 2H), 7.78 (dd, J = 6.1, 3.2 Hz, 2H), 7.76 – 7.45 (m, 12H), 7.34 (dd, J = 6.2, 3.4 Hz, 2H), 6.82 (dd, J = 6.2, 3.3 Hz, 2H). Primary m/z peak calculated $C_{44}H_{26}$: 554.20, found: 554.20.

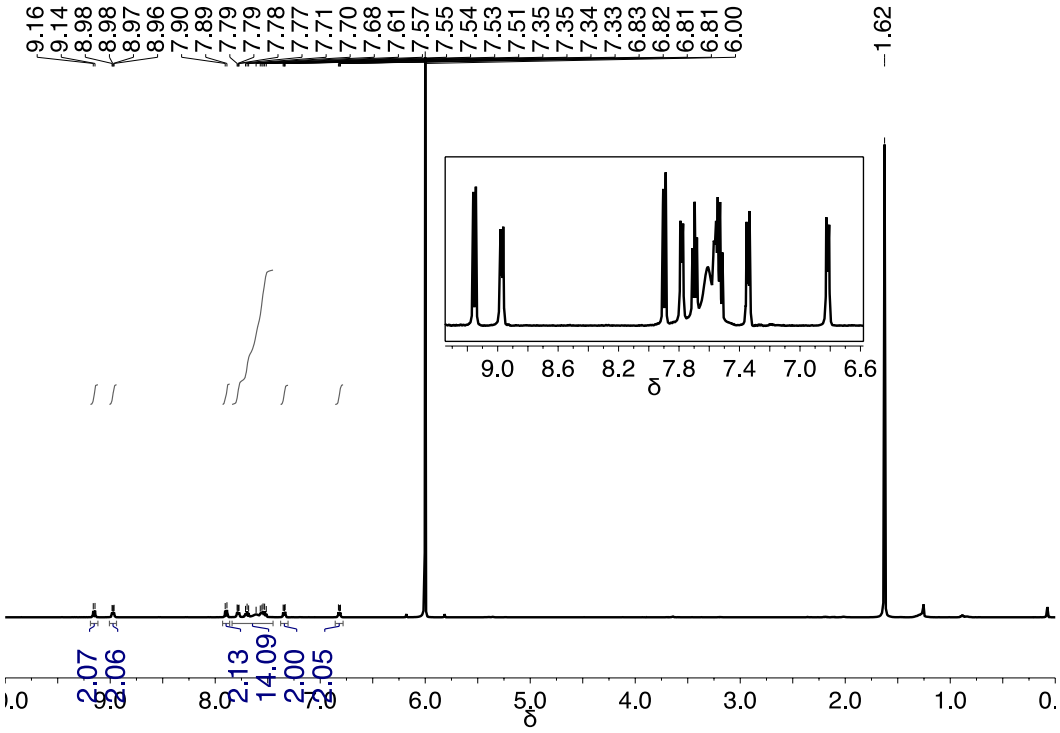

Figure S21. ^{1}H NMR of 13,18-diphenylbenzonaphtho[1,2,3,4]pentaphene (9). Peaks assigned to molecule have been expanded in the inset figure.

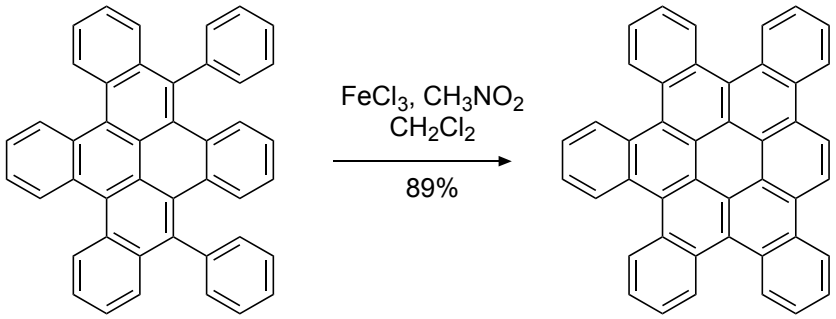

9 **10**

Synthesis of (10) pentabenzocoronene

Synthesis of **10** also required the use of a Scholl ring closure, as used for 5, above. Starting with 90 mg (0.16 mmol) of **9**, resulted in 79 mg of yellow powder of **10** after workup (89% yield). ^{1}H NMR (500 MHz, Tetrachloroethane-d_2) δ 9.39 (s, 2H), 9.32 (d, J = 8.0 Hz, 4H), 9.28 – 9.23 (m, 4H), 9.18 (d, J = 7.8 Hz, 2H), 7.99 – 7.85 (m, 8H), 7.83 (t, J = 7.3 Hz, 2H). Primary m/z peak calculated $C_{44}H_{22}$: 550.17, found: 550.19.

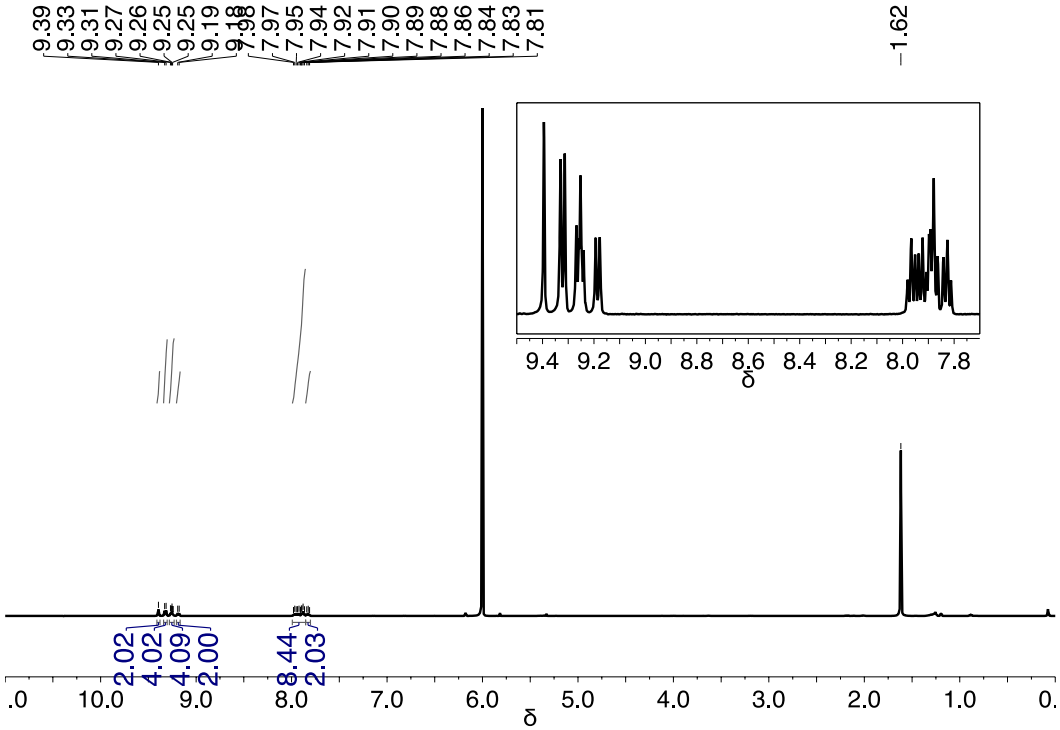

Figure S22. ^{1}H NMR of cPBC (10). Peaks assigned to molecule have been expanded in the inset figure.

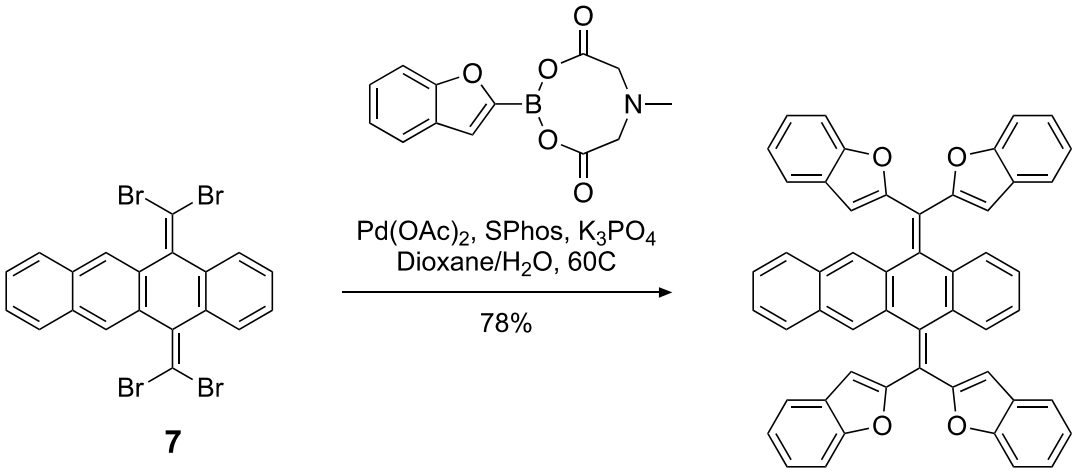

7 **11**

Synthesis of (11) 5,12-bis(di(benzofuran-2-yl)methylene)-5,12-dihydrotetracene (Suzuki coupling)

Suzuki coupling to produce **11** closely follows the procedure used previously by Davy et al., which utilized N-methyliminodiacetic acid (MIDA) boronates instead of boronic acid derivatives[9]. 140 mg (0.25 mmol) of **7**, 11 mg (0.05 mmol) of palladium(II) acetate, 40.3 mg (0.10 mmol) of 2-Dicyclohexylphosphino-2′,6′-dimethoxybiphenyl (SPhos), and 335.5 mg (1.25 mmol) of benzofuranyl-2-boronic acid MIDA ester were added to a nitrogen-purged, 25 mL roundbottom flask and purged with nitrogen. Dioxane (12.5 mL) was added via syringe to the roundbottom flask and sparged with nitrogen for 20 minutes. (391 mg, 1.8 mmol) tribasic postassium phosphate were added to a 20 mL vial and sealed with a septum. 2 mL of distilled H2O were added via syringe to the vial containing the base and were sparged with nitrogen for 20 minutes. The vial was then lowered into a silicon oil bath heated to 60C, and the base solution was added via needle through the septa. The solution was sparged for 5 minutes before the inlet and outlet were removed and the reaction was stirred overnight. The reaction was stopped when **7** was consumed (verified by TLC hexanes/DCM 3:1) and the solution became brown. The product was then extracted with dichloromethane, separated from the aqueous phase, washed with brine solution, and extracted with dichloromethane and separated again. The organic phase was then dried via rotovap, purified using flash column chromatography (hexane/DCM 3:1) and crystallized in solution using dichloromethane/methanol to isolate 165 mg (80%) of **11**. ^{1}H NMR (500 MHz, Methylene Chloride-d_2) δ 7.95 (s, 2H), 7.60 – 7.19 (m, 22H), 7.02 (dd, J = 5.8, 3.2 Hz, 2H), 6.76 (d, J = 17.0 Hz, 4H). ^{13}C NMR (126 MHz, CD_2Cl_2) δ 155.15, 142.42, 137.99, 134.68, 132.31, 128.41, 127.58, 127.41, 127.11, 126.65, 125.25, 123.54, 121.69, 118.62, 111.71, 108.78, 108.49. Primary m/z peak calculated $C_{52}H_{30}O_4$: 718.21, found: 718.22.

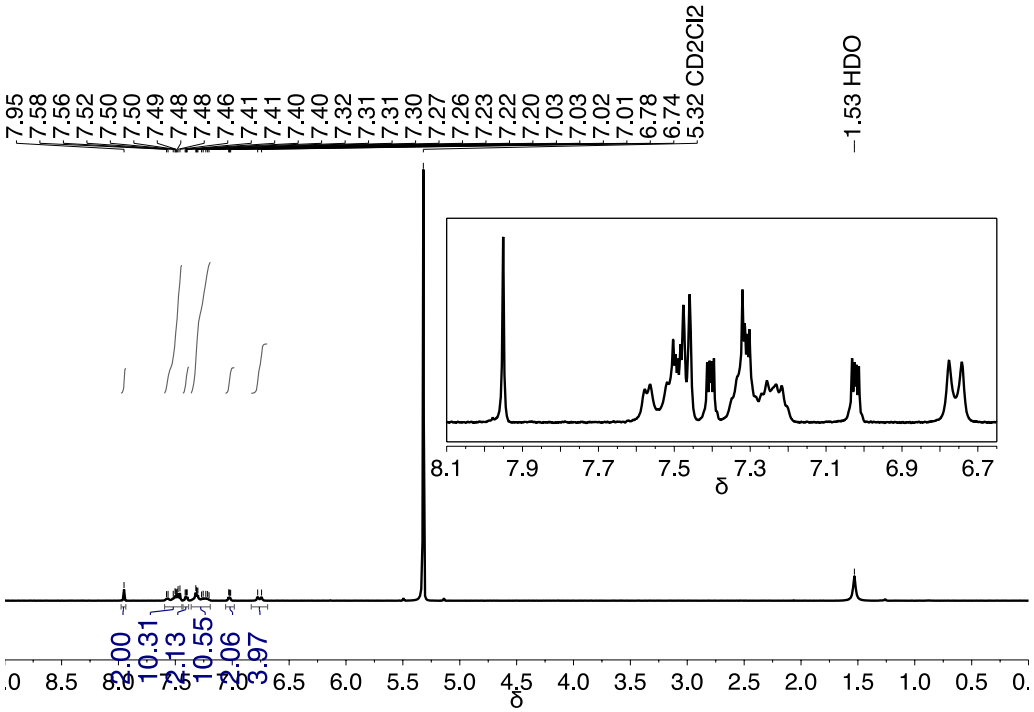

Figure S23. ^{1}H NMR of 5,12-bis(di(benzofuran-2-yl)methylene)-5,12-dihydrotetracene (11). Peaks assigned to molecule have been expanded in the inset figure.

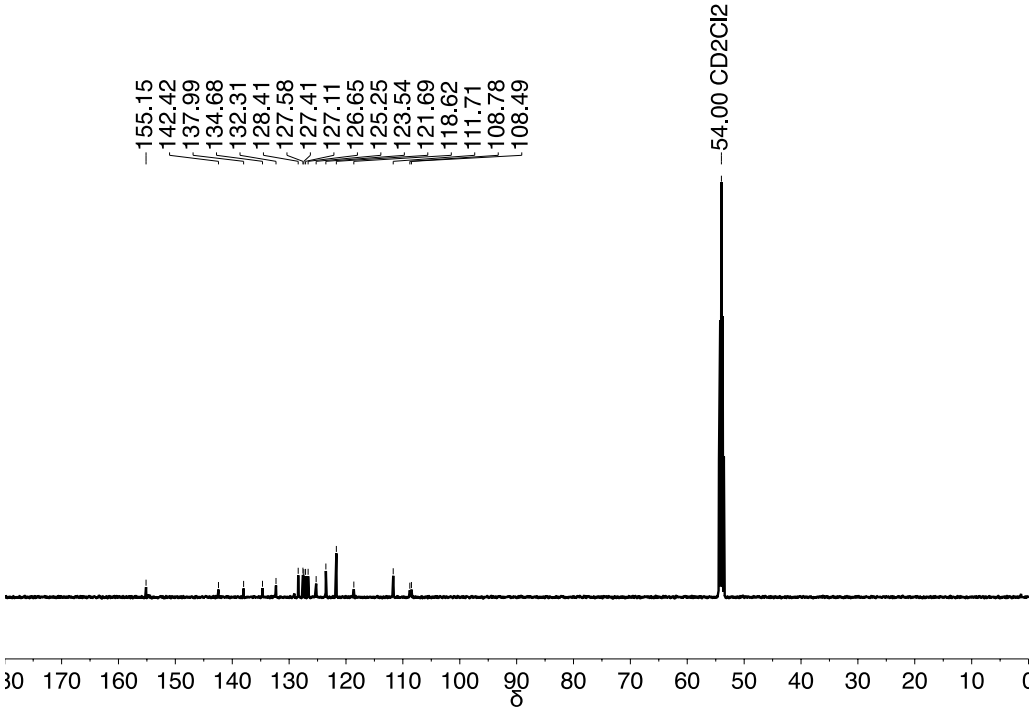

Figure S24. ^{13}C NMR of 5,12-bis(di(benzofuran-2-yl)methylene)-5,12-dihydrotetracene (11).

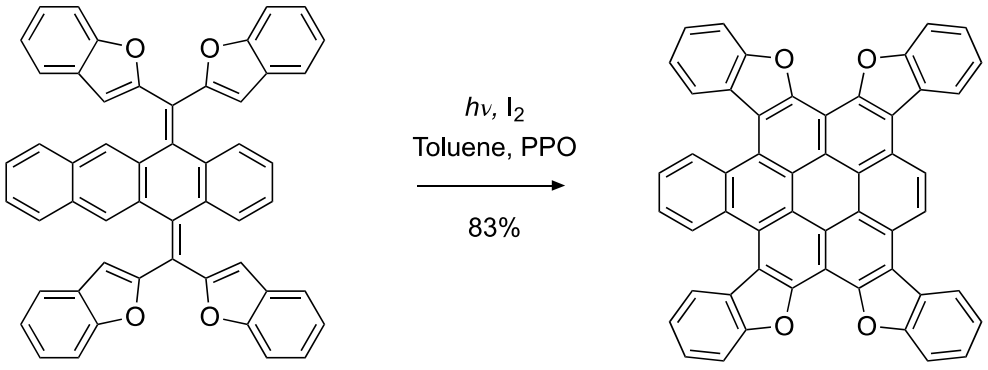

11 **12**

Synthesis of (12) cTBFBC (benzo[3,4]benzo[4',5']furan[3',2':5,6]-benzo[4',5']furan[2',3':7,8] benzo[4',5']furan- [3',2':11,12]coroneno[1,2-b]benzofuran)

Synthesis of **12** followed the same photocyclization procedure as that for **4** and **10**, above, and closed fully through photocyclization. Starting with 75 mg (0.10 mmol) of **11**, resulted in 62 mg of yellow powder of **8** after workup (83% yield) which produced green fluorescence on the TLC plate. ^{1}H NMR (500 MHz, 1,2-Chlorobenzene-d_4) δ 9.81 (dd, J = 6.0, 3.6 Hz, 2H), 9.75 (s, 2H), 9.05 (d, J = 7.9 Hz, 2H), 8.89 (d, J = 7.5 Hz, 2H), 8.14 – 8.08 (m, 4H), 7.96 (d, J = 6.8 Hz, 2H), 7.72 – 7.62 (m, 6H), 7.58 (t, J = 7.4 Hz, 2H). Primary m/z peak calculated $C_{52}H_{22}O_4$: 710.15, found: 710.15.

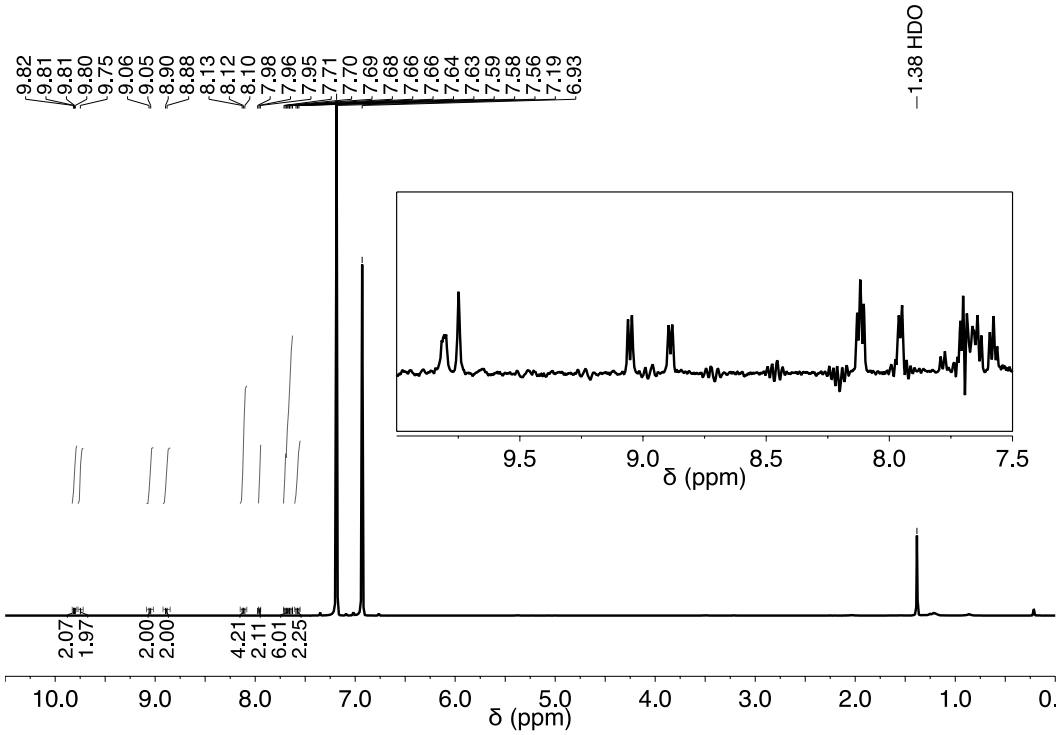

Figure S25. ^{1}H NMR of cTBFBC (12). Peaks assigned to molecule have been expanded in the inset figure.

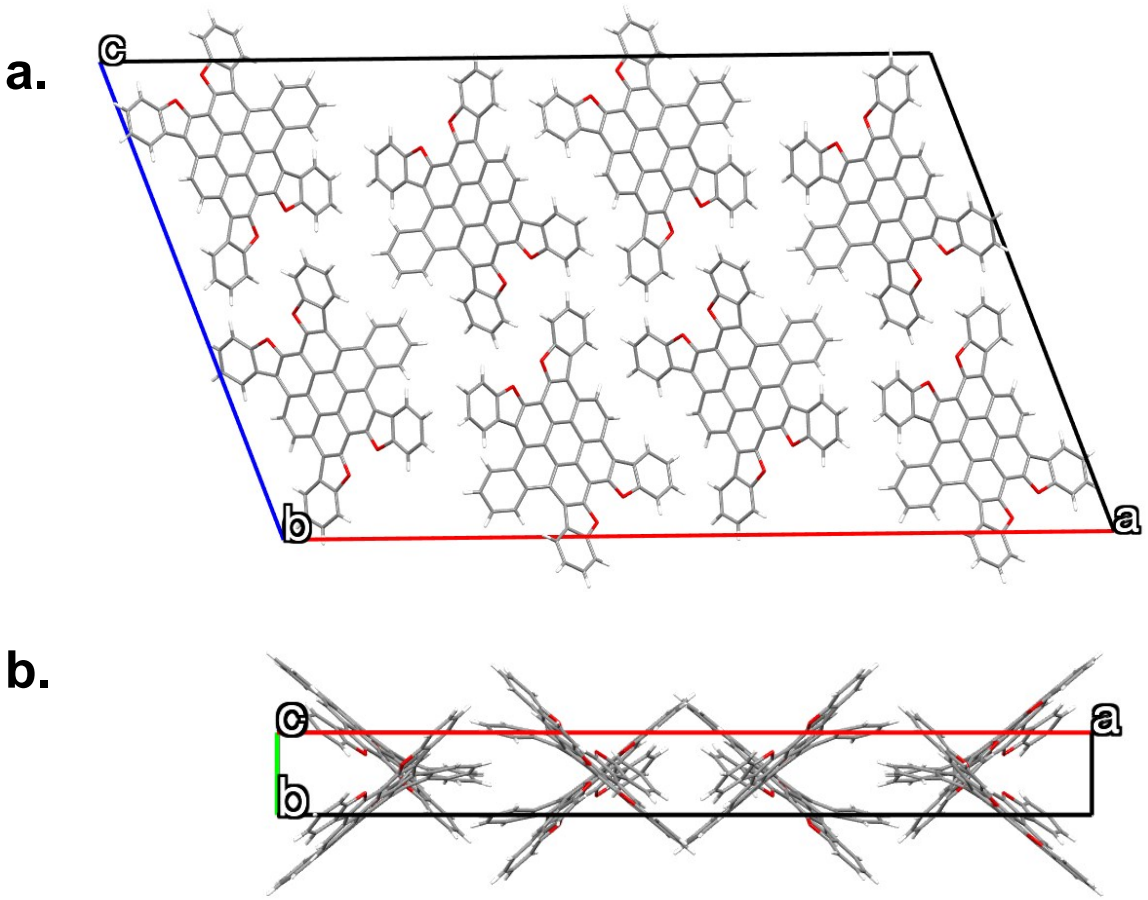

Figure S26. Single crystal structure of cTBFBC. (a) View along the b-axis of the unit cell. (b) View along the c-axis of the unit cell. Structure is deposited as CCDC 2040902.

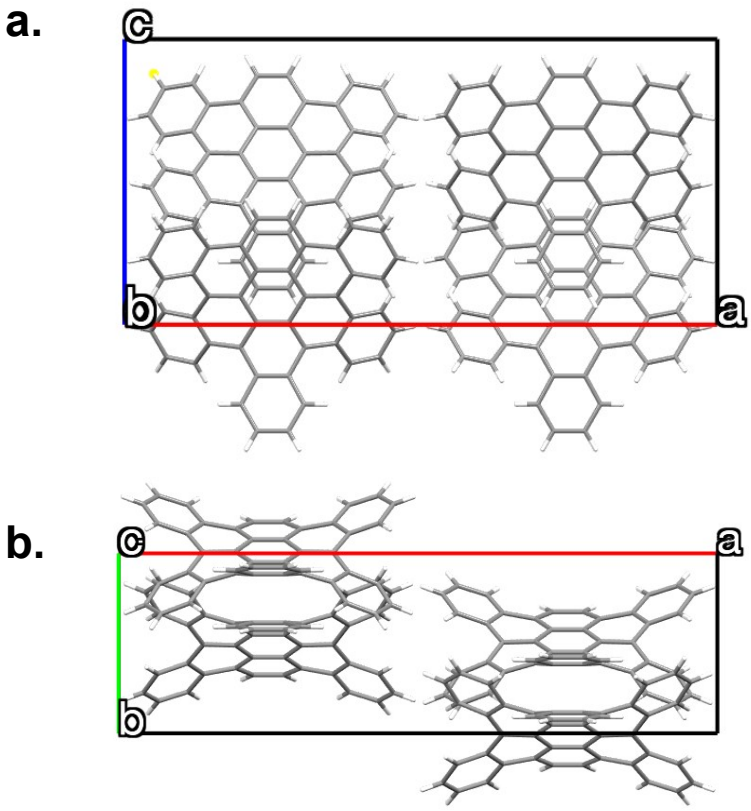

Figure S27. Single crystal structure of cPBC. (a) View along the b-axis of the unit cell. (b) View along the c-axis of the unit cell. Structure is deposited as CCDC 2040903.

References

1 A. M. Hiszpanski, J. D. Saathoff, L. Shaw, H. Wang, L. Kraya, F. Lüttich, M. A. Brady, M. L. Chabinyc, A. Kahn, P. Clancy and Y.-L. Loo, *Chem. Mater.*, 2015, **27**, 1892–1900.

2 S. A. Lopez, E. O. Pyzer-Knapp, G. N. Simm, T. Lutzow, K. Li, L. R. Seress, J. Hachmann and A. Aspuru-Guzik, *Sci. Data*, 2016, **3**, 1–7.

3 P. Pracht, F. Bohle and S. Grimme, *Phys. Chem. Chem. Phys.*, 2020, **22**, 7169–7192.

4 A. D. Becke, *Phys. Rev. A*, 1988, **38**, 3098–3100.

5 F. Weigend and R. Ahlrichs, *Phys. Chem. Chem. Phys.*, 2005, **7**, 3297–3305.

6 A. D. Becke, *J. Chem. Phys.*, 1993, **98**, 5648–5652.

7 C. I. Wu, Y. Hirose, H. Sirringhaus and A. Kahn, *Chem. Phys. Lett.*, 1997, **272**, 43–47.

8 K. N. Plunkett, K. Godula, C. Nuckolls, N. Tremblay, A. C. Whalley and S. Xiao, *Org. Lett.*, 2009, **11**, 2225–2228.

9 N. C. Davy, G. Man, R. A. Kerner, M. A. Fusella, G. E. Purdum, M. Sezen-Edmonds, B. P. Rand, A. Kahn and Y.-L. Loo, *Chem. Mater.*, 2016, **28**, 673–681.